ChemPubSoc Europe

DOI: 10.1002/chem.201603938

CHEMISTRY A European Journal Full Paper

Supramolecular Polymerization

Unravelling the Pathway Complexity in Conformationally Flexible *N*-Centered Triarylamine Trisamides

Beatrice Adelizzi,[a, b] Ivo A. W. Filot,[c] Anja R. A. Palmans,*[a, b] and E. W. Meijer*[a, b]

Abstract: Two families of C_3-symmetrical triarylamine-trisamides comprising a triphenylamine- or a tri(pyrid-2-yl)amine core are presented. Both families self-assemble in apolar solvents via cooperative hydrogen-bonding interactions into helical supramolecular polymers as evidenced by a combination of spectroscopic measurements, and corroborated by DFT calculations. The introduction of a stereocenter in the side chains biases the helical sense of the supramolecular polymers formed. Compared to other C_3-symmetrical compounds, a much richer self-assembly landscape is observed. Temperature-dependent spectroscopy measurements highlight the presence of two self-assembled states of opposite handedness. One state is formed at high temperature from a molecularly dissolved solution via a nucleation–elongation mechanism. The second state is formed below room temperature through a sharp transition from the first assembled state. The change in helicity is proposed to be related to a conformational switch of the triarylamine core due to an equilibrium between a 3:0 and a 2:1 conformation. Thus, within a limited temperature window, a small conformational twist results in an assembled state of opposite helicity.

Introduction

Triarylamine-based molecules are widely studied in organic electronics for their versatile properties.[1–12] For attaining good conductive properties, it is crucial to achieve a well-organized microstructure in which defects and localized electronic states are minimized.[13,14] Recent research demonstrates that the ability to exert full control during the formation of the desired nanostructures enhances the performance of functional materials. This control can be achieved by applying a supramolecular approach for the preparation of functional materials.[15–21] For example, Giuseppone and co-workers studied in detail the self-assembly of *N*-centered triphenylamine-trisamide in apolar solvents and the photo-induced supramolecular polymerization upon oxidation of triphenylamine into triphenylammonium in the presence of chloroform.[22,23] The improved conductive properties, in combination with easy processability, highlight that self-assembly is an attractive strategy to achieve well-performing supramolecular electronics.[24,25] In addition, Seu and Kim have demonstrated that opposite helical senses in photo-oxidized triphenylamine stacks can be induced by applying circularly polarized light of opposite handedness, opening a new route towards the formation of supramolecular chiral conductors.[26]

However, supramolecular interactions do not always result in the formation of thermodynamically stable states. Pathway complexity—the different reaction pathways and intermediates that can occur in a self-assembling system—has recently been disclosed in several systems and the importance of controlling complex kinetic processes is a fundamental next step to take.[27–30] The ability to access different assembled states and the quantification of the energetic barriers of a complex supramolecular landscape creates opportunities to realize living supramolecular polymerizations.[31–34] Initially the strategy used to control the assembled architectures was the isolation of a kinetically trapped state and its seeding with a thermodynamically stable aggregate seed.[31,35] However, recently Aida[36] and Würthner [32,37] have improved the control through rationally designed monomers that can be tuned ad hoc to polymerize in a controlled fashion. Their approaches suggest the importance of a certain degree of conformational freedom within the molecules to obtain responsive monomers that are sensitive to stimuli such as initiator,[36] light,[22] solvent,[38,39] or temperature. Understanding pathway complexity, as suggested by Mukhopadhyay and Ajayaghosh,[40] is now a tool to design

[a] *B. Adelizzi, Dr. A. R. A. Palmans, Prof. Dr. E. W. Meijer*
Laboratory of Macromolecular and Organic Chemistry
Eindhoven University of Technology
Eindhoven (The Netherlands)
E-mail: E.W.Meijer@tue.nl

[b] *B. Adelizzi, Dr. A. R. A. Palmans, Prof. Dr. E. W. Meijer*
Institute for Complex Molecular Systems,
Eindhoven University of Technology
Eindhoven (The Netherlands)

[c] *Dr. I. A. W. Filot*
Institute of Catalysis
Eindhoven University of Technology
Eindhoven (The Netherlands)

Supporting information for this article can be found under: http://dx.doi.org/10.1002/chem.201603938.

functional materials. This combination will be a fundamental step forward in high-performance soft electronics.

In this work, we present a study on the control and pathway selection on the self-assembly of two triarylamine families and report the importance of conformational flexibility. We show how a small energetic gap in the molecular conformation can play an essential role in the resulting assembled state, leading to a fast inversion of helical bias as a function solely of the temperature.

The two selected cores, the classic triphenylamine and the tri(pyrid-2-yl)amine, possess the same geometry but different electronic properties and intermolecular interactions. The monomer structures are designed with a classical C_3 symmetry, similar to the benzene-1,3,5-tricarboxamides (BTAs),[41,42,43] with an aromatic core, a C=O centered three-folded H-bonding unit and alkyl-solubilizing chains (Scheme 1). The conjugation between the central donating nitrogen and the amide moieties is enhanced in the triphenylamine, whereas the electron-poor pyridyl group modifies the conjugation. Unlike the triphenylamine core, the assembly properties of tri(pyrid-2-yl)amine are unexplored but the good flexibility of the molecule is known and exploited in various metal complexes and chiral molecular organic nanotubes (MONTs).[44,45,46]

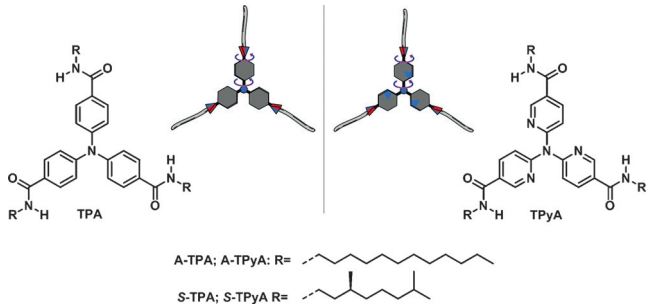

Scheme 1. Chemical structures of tri-*p*-carboxamides triphenylamine (with achiral C12 chain **A-TPA** and with (*S*)-dimethyloctyl chain ***S*-TPA**) and tri-5-carboxamides tri(pyrid-2-yl)amine (with achiral C12 chain **A-TPyA** and with (*S*)-dimethyloctyl chain ***S*-TPyA**).

Results and Discussion

Synthesis and solid-state properties

The synthetic approach to access trialkyl-substituted carbonyl-centered triphenylamine-trisamides (TPAs) and tripyridylamine-trisamides (TPyAs) is depicted in Scheme 2. The carboxylic acid precursors were synthesized by using procedures described in literature.[47,45] The amide coupling was performed with both achiral dodecylamine (**A-TPA** and **A-TPyA**) and chiral (*S*)-3,7-dimethyloctylamine (***S*-TPA** and ***S*-TPyA**).

TPAs were obtained by first converting the tricarboxylic triacid into the triacid trichloride using oxalyl chloride, followed by coupling to the desired amines (dodecylamine and (*S*)-3,7-dimethyloctylamine).[48] For the TPyAs, in contrast, the acyl chloride intermediate was unstable and therefore the amide coupling was achieved by activation of the triacid by CDI coupling.[45] After purification by column chromatography and recrystallization, all TPAs and TPyAs were obtained in high purity as verified by ^{1}H and ^{13}C NMR spectroscopy and MALDI-TOF-MS. The bulk properties of synthesized triarylamines were fully evaluated by performing differential scanning calorimetry (DSC) and polarized optical microscopy (POM). The presence of a hydrogen-bonding framework between amides was verified through temperature-dependent infrared (IR) spectroscopy (see Figures S1–S8 and Tables S1 and S2 in the Supporting Information,).

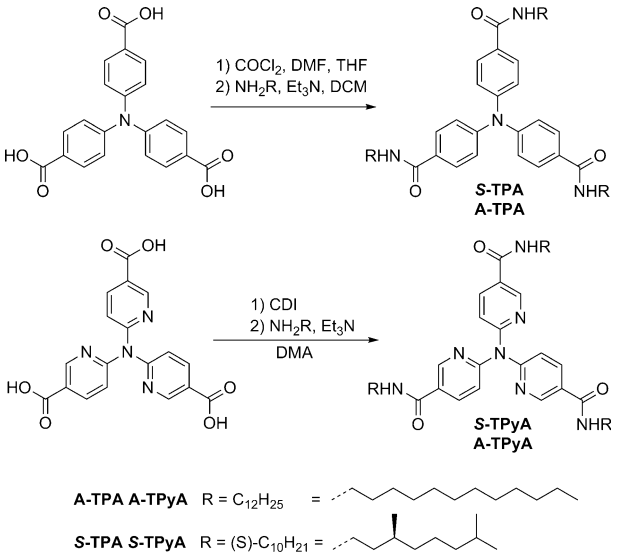

Scheme 2. Amide coupling of TPA and TPyA with achiral (**A-TPA** and **A-TPyA**) and (*S*) chiral chains (***S*-TPA** and ***S*-TPyA**).

Self-assembly in methylcyclohexane

The self-assembly processes of the trisamides are sensitive to changes in molecular environment, which affects the electronic transitions. Both trisamides were studied by using temperature-dependent spectroscopic measurements in methylcyclohexane (MCH) and chloroform. In chloroform, all trisamides are molecularly dissolved, whereas apolar solvents such as MCH, promote self-assembly at room temperature via directional hydrogen bonding. This is evidenced by changes in the optical properties upon cooling as a result of supramolecular polymerization in MCH, which is not present in chloroform at these concentrations (see Figure S9 in the Supporting Information). The absorption and emission spectra of a 5×10^{-5} M solution in MCH of ***S*-TPA** and ***S*-TPyA** were measured in a temperature range between 373.5 and 298.5 K (see Figure S10 in the Supporting Information).

The thermal treatment of both molecules shows a blue-shifted absorption upon cooling with a blue-shifted shoulder arising and a quenched red-shifted emission; these variations can be attributed to an aggregation process that affects the energy levels of the entire molecule. However, understanding the aggregation processes involved is arduous even if the transitions appear rather clear. Moreover, the intensity plots of the spectroscopic maxima show a non-linear trend. Thus, with the

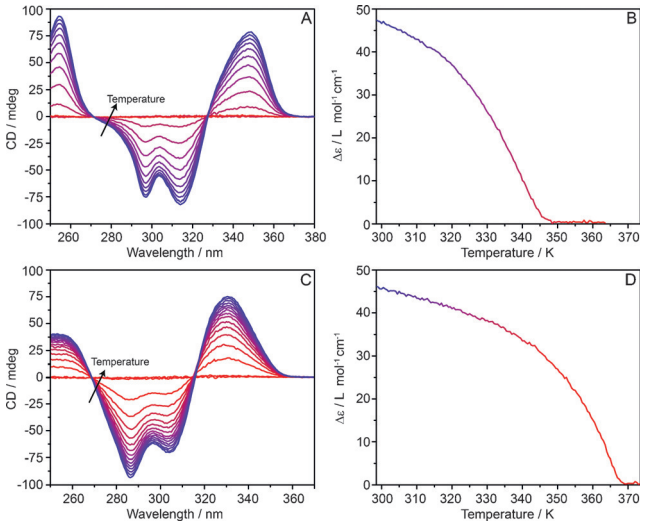

Figure 1. CD spectra of ***S*-TPA** (A) and ***S*-TPyA** (C) in MCH ($c = 5 \times 10^{-5}$ M). CD spectra recorded every 5 K. Molar circular dichroism as a function of temperature monitored at $\lambda = 347$ nm for ***S*-TPA** (B) and at $\lambda = 331$ nm for ***S*-TPyA** (D) ($c = 5 \times 10^{-5}$ M).

aim of better defining the processes we acquired circular dichroism (CD) spectra over a broad temperature range (Figure 1).

Owing to the chirality of the monomer that imposes a preferred helicity to the supramolecular aggregate, we investigated the aggregation in these macromolecular helical assemblies. Both systems display no CD effect at high temperature, while upon cooling and aggregation a strong positive Cotton effect is recorded in the triarylamine absorption bands around $\lambda =$ 347 nm for ***S*-TPA** and $\lambda = 331$ nm ***S*-TPyA**, respectively. The positive Cotton effect recorded upon aggregation for both samples indicates that the chirality of the chains dominates the sign and shape of the CD regardless of the structure of the central core. This finding shows that the main driving force of the polymerization is the hydrogen-bond interaction. To probe the evolution in detail, the molar circular dichroism ($\Delta\varepsilon$) in the maximum Cotton effect was monitored as a function of temperature. The experimental melting curves were recorded starting at high temperature in a molecularly dissolved solution and cooled down at 60 K h^{-1}. The melting curves recorded show two regimes, an initial phase at high temperature where no long aggregates are formed, characterized by no CD effect, followed by a sharp transition to positive CD values that occurs at 348.7 K for ***S*-TPA** and 368.5 K for ***S*-TPyA**, respectively. The transition temperatures reveal that ***S*-TPyA** shows the formation of aggregates very close to the boiling point of the solvent at $c = 5 \times 10^{-5}$ M and that ***S*-TPA** starts to polymerize at a temperature 20 K lower than ***S*-TPyA**. The melting curves were also recorded at different concentrations and a shift of the elongation temperature (T_e) to higher temperatures was observed upon increasing the concentration (see Figure S11 in the Supporting Information). These results confirm that both the triarylamines exhibit a strongly cooperative polymerization in alkane solvents. The van't Hoff plot for ***S*-TPA** and ***S*-TPyA** showed a larger thermodynamic gain upon aggregation of ***S*-TPyA** than ***S*-TPA**, which is in agreement with the higher T_e observed at $c = 5 \times 10^{-5}$ M (Table 1).

Table 1. Molar circular dichroism $\Delta\varepsilon$ of ***S*-TPA** and ***S*-TPyA** at 298.5 K at 50 μM monitored at $\lambda = 347$ nm and $\lambda = 331$ nm, respectively, and thermodynamic parameters obtained by the van't Hoff plot.

	$\Delta\varepsilon$ [L mol^{-1} cm^{-1}]	T_e [K]	ΔH (R^2)[a] [kJ mol^{-1}]
***S*-TPA**	47.41	348.3	−77.18 (0.99)
***S*-TPyA**	46.15	368.5	−125.14 (0.99)

[a] Derived from the van't Hoff plot of ***S*-TPA** and ***S*-TPyA** in MCH ($c = 5$ 10^{-5} M).

In a more detailed analysis, we fitted the melting curves to the nucleation–elongation model developed by Markvoort et al.[49] to calculate the released enthalpy upon elongation. Interestingly, we observe that for both the triarylamines the model does not fit properly showing a significant deviation in the multicurve fit (see Figures S18 and S19 in the Supporting Information). The deviation from a classic cooperative model is coherent with the trends recorded in the temperature-dependent UV/Vis and fluorescence measurements and clearly indicates that a second process competes in the nucleation–elongation polymerization at lower temperatures.

Self-assembly behavior below room temperature

Motivated to have a clearer and wider view, we investigated the self-assembly behavior in MCH solution by reducing the temperature. UV/Vis and emission spectra at 263.5 K are depicted and compared with the data recorded at 323.5 K in the first assembled state and at 368.5 K in the monomerically dissolved state (Figure 2). The temperature-dependent measurements show another unexpected transition at 273.5 K and

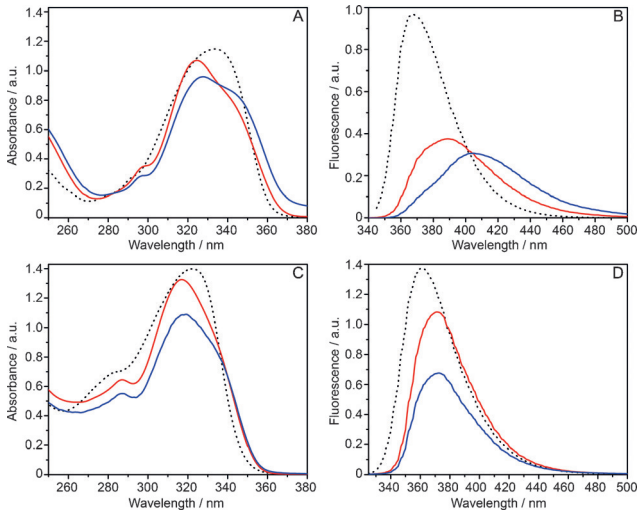

Figure 2. UV/Vis and fluorescence spectra of ***S*-TPA** (A, B) and ***S*-TPyA** (C, D) in MCH ($c = 5 \times 10^{-5}$ M). Dotted black lines, monomerically dissolved solutions (363.5 K ***S*-TPA** and 373.5 K ***S*-TPyA**). Red lines, spectra recorded at 323.5 K, blue lines, spectra recorded at 263.5 K.

288.5 K for ***S*-TPA** and ***S*-TPyA**, respectively (see Figures S12–S15 in the Supporting Information).

At 263.5 K ***S*-TPA** shows an evident increment of the red-shifted shoulder at 350 nm, whereas the main peak and the blue-shifted shoulder decrease. Similarly, the fluorescence displays a 20 nm red-shift of the aggregate peak, whereas the monomer fluorescence almost completely vanishes. In contrast, the change in shape is not so drastic for ***S*-TPyA**, both absorbance and fluorescence spectra at 263.5 K show a decrease in intensity.

We repeated the analysis by measuring the evolution of the CD as a function of temperature. The CD effect was probed at $\lambda = 347$ nm for ***S*-TPA** and $\lambda = 331$ nm for ***S*-TPyA** and data were recorded starting at high temperature in a molecularly dissolved solution and cooling down the solution at 60 K h^{-1}. After a short equilibration at 263.5 K the system was heated with the same rate (Figure 3). Interestingly, the cooling curve

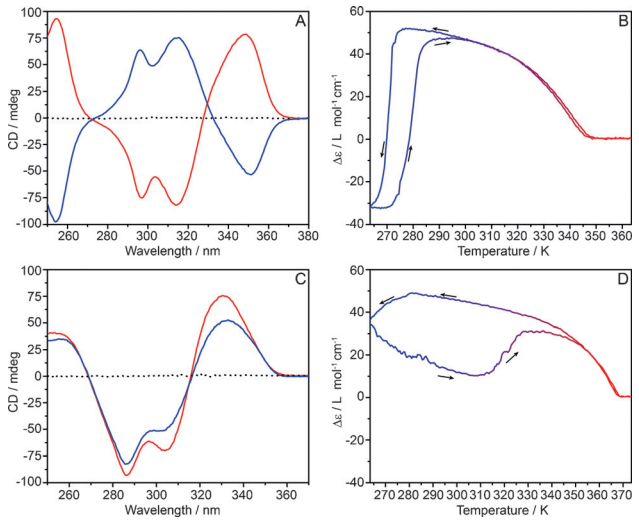

Figure 3. CD spectra of ***S*-TPA** (A) and ***S*-TPyA** (C) in MCH ($c = 5 \times 10^{-5}$ M). Dotted black lines represent the CD spectrum of the monomerically dissolved solutions. Red lines are the spectra recorded at 323.5 K, blue lines are the spectra recorded at 263.5 K. Melting curves of ***S*-TPA** (B) and ***S*-TPyA** (D) at a cooling–heating rate of 60 K h^{-1}.

for ***S*-TPA** exhibits a pronounced inversion of the Cotton effect at 273.5 K leading to negative values at 263.5 K. Upon heating, the curve is not superimposable with the cooling curve. The negative Cotton effect persists for 10 K and shows a drastic inversion around 273.5 K. Above 298.5 K the two curves are superimposable again. Fascinatingly, the shape of the CD spectra at high and low temperatures are nearly mirror images displaying a shift of a few nanometers only. For ***S*-TPyA** the CD intensity recorded below 273.5 K shows just a small decrease combined with a small red-shift. The cooling curve reveals an inversion in the trend around 283.5 K. Differently from the triphenylamine, no opposite Cotton effect is observed. However, upon heating a large hysteresis effect is observed that disappears just above 350.5 K.

The changes in the CD spectra and other spectroscopic measurements suggest that a transition within the aggregated state occurs below room temperature. Whereas ***S*-TPyA** displays distinct changes in all spectra, the thermal treatment on ***S*-TPA** promotes even an inversion of handedness. Due to the similarities between the two triarylamines we speculated on the possibility that they show analogous behavior. Therefore, we studied the self-assembly of ***S*-TPyA** in decalin (mixture of isomers) in order to decrease the strength of the interaction among monomers and solvent. The solubility of ***S*-TPyA** in decalin is better than that in MCH and the thermodynamic parameters of ***S*-TPyA** in decalin are closer to the values of ***S*-TPA** in MCH (see Figure S15 and Table S4 in the Supporting Information). The recorded spectra and the cooling/heating curve of ***S*-TPyA** in decalin are indeed more similar to those of ***S*-TPA** in MCH (Figure 4). The absorption peak of ***S*-TPyA** in decalin

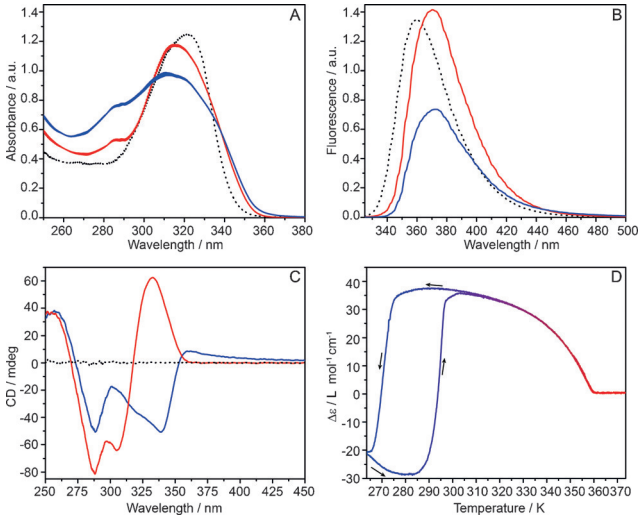

Figure 4. Recorded spectra of ***S*-TPyA** in decalin isomers mixture ($c = 5 \times 10^{-5}$ M), respectively, UV/Vis (A), fluorescence (B), CD spectra (C), and relative melting curve monitored at $\lambda = 333$ nm at a cooling-heating rate of 15 K h^{-1}. D) Dotted black lines represent the CD spectrum of the monomerically dissolved solutions recorded at 373.5 K. Red lines are the spectra recorded at 323.5 K, blue lines are the spectra recorded at 263.5 K.

shows a general broadening at 263.5 K with an evident increment of the blue-shifted shoulder and a decrease of main peak. Similarly to what was observed in MCH, the fluorescence is half-quenched. The CD melting curves at $\lambda = 333$ nm display the same handedness and cooperativity than those in MCH but, below room temperature a sharp inversion results in opposite CD values like ***S*-TPA** in MCH.

The hysteresis recorded in the heating curve is around 30 K. Nevertheless, unlike for its triphenylamine analogue, the ***S*-TPyA** CD spectra below and above room temperature have a different shape: the inversion of the bisignated CD is only partial, the high-energy couplet displays just a small decrease while the peaks above 300 nm are inverted. Moreover, the low-temperature spectrum shows a small positive Cotton effect at 350 nm that can probably be assigned to the presence of large aggregates that scatter the light since almost no absorption is recorded in that region (this hypothesis is supported by DLS data, Figure S17 in the Supporting Information).

Computational Analysis

To better analyze the systems, DFT calculations were performed. To reduce the computational time, calculations were performed on oligomers and infinite chains of TPA and TPyA, in which the aliphatic chains are replaced by a methyl group. Upon supramolecular aggregation, TPA and TPyA monomers can self-assemble in such a way that the hydrogen-bonding dipoles either align in a parallel or in an *anti*-parallel fashion. The dipole moments are oriented from the carbonyl oxygen of one discotic to the amide hydrogen of a neighboring discotic. Herein, we refer to these two different conformations as 3:0 (where all three dipoles are parallel) and 2:1 (two parallel and one antiparallel), respectively.[50] The calculated structures of TPA and TPyA for these two possible conformations are reported in Figure 5 and Figure 6, while the discussion of the data is reported in the computational analysis section of the Supporting Information.

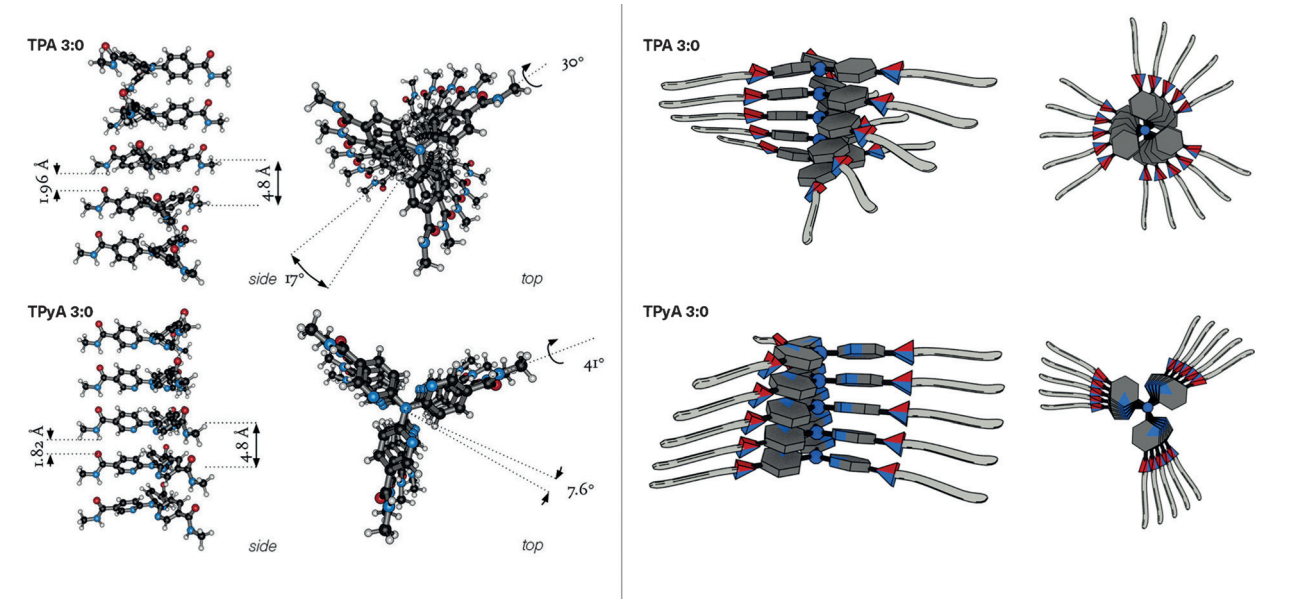

Figure 5. Three-dimensional structure of triphenylamine (TPA, top) and tripyridylamine (TPyA, bottom) for the 3:0 conformation (parallel orientation of the dipoles). On the left, DFT calculated structures. The interdiscotic distance, d_D, and angle, α, the hydrogen bond length, d_H, and the carbonyl-phenyl/pyridyl dihedral angle, θ, are given. On the right, cartoons are reported to represent the molecular organization.

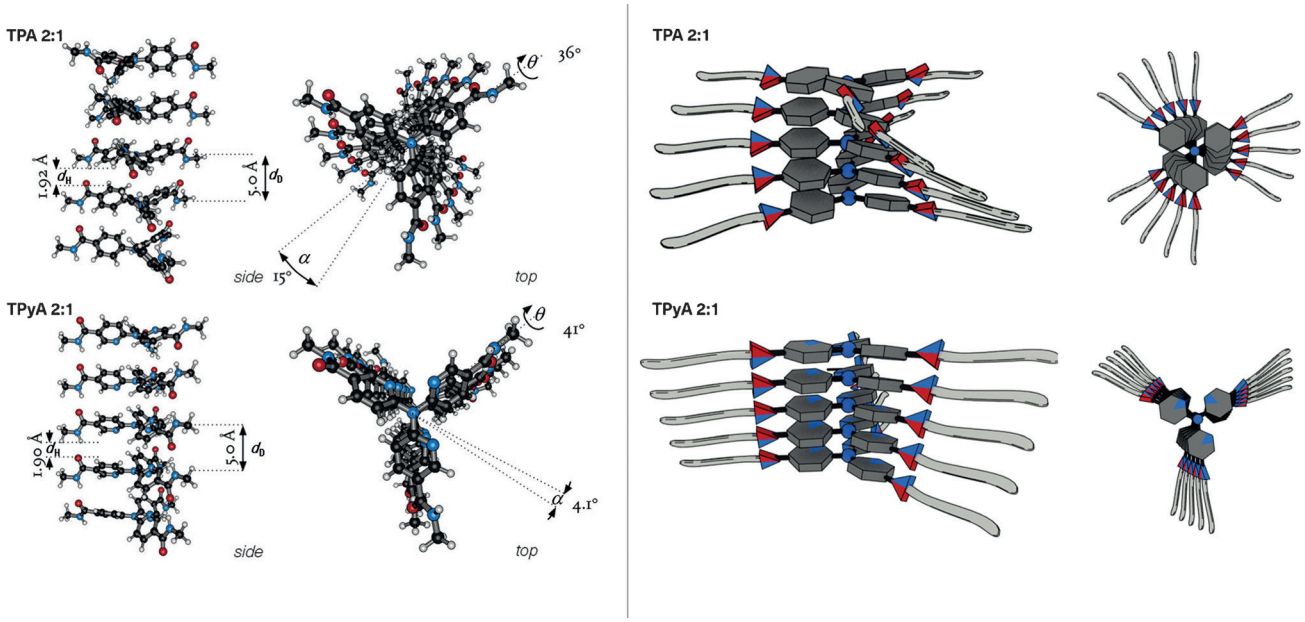

Figure 6. Three-dimensional structure of triphenylamine (TPA, top) and tripyridylamine (TPyA, bottom) for the 2:1 conformation (*anti*-parallel orientation of the dipoles). On the left, DFT calculated structures. The interdiscotic distance, d_D, and angle, α, the hydrogen bond length, d_H, and the carbonyl-phenyl/pyridyl dihedral angle, θ, are given. On the right, cartoons are reported to represent the molecular organization.

Interestingly, for TPyA the inversion of the amide between 3:0 and 2:1 occurs with a coherent torsion of the pyridine ring in order to maintain the antiparallel orientation of the pyridine dipole and amide dipole. Thus the conformation 2:1 of TPyA loses the C_3 symmetry of the triarylamine core. In both the conformational states, TPyA shows a carbonyl dihedral angle (θ) moderately larger compared to TPA and BTA.[51] The greater rotational mobility of the carbonyl group is rationalized by the deactivation of the conjugated π-system by the presence of the nitrogen in the pyridyl ring. As the pyridyl nitrogen withdraws electronic density from the π-system, less overlap between the latter and the carbonyl group results in an enhanced rotational flexibility. This greater torsion is reflected in a smaller interdiscotic angle (α) and hydrogen bond length (d_H) compared to TPA.

Therefore, the carbonyl groups of TPyA have a higher out-of-plane rotation resulting in a more favorable conformation for hydrogen bond formation leading to a stronger interaction energy (Figures 5, Figure 6, Figure 7). Regardless of the number of monomers in the supramolecular chain and the conformation assumed, the binding energy is larger (i.e., more stable) for TPyA aggregates compared to the TPA aggregates, corroborating our experimental observations (Table 1). Furthermore, the binding energy analysis reveals that the supramolecular polymerization is cooperative, that is, the consecutive addition of monomers to the supramolecular aggregate results in an increasingly stronger binding energy between the monomers. For both the molecules, the antiparallel conformation (2:1) in the oligomer is more stable. The infinite chain calculation follows the same trend.

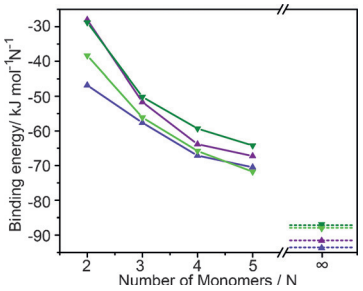

Figure 7. Average binding energy per monomer for the dimer up to and including the pentamer of tripyridylamine (TPyA, bordeaux ▲ for 3:0 and purple ▲ for 2:1) and triphenylamine (TPA, dark green ▼ for 3:0 and light green ▼ for 2:1) for both the 3:0 and 2:1 conformations. The dotted lines depict the asymptotic value of the average binding energy of the periodic chains. All energies are given in kJ mol^{-1}.

State analysis

The thermal analysis performed on both systems highlights a general behavior. A first assembled state (state A), with positive CD extrema at $\lambda = 347$ nm for ***S*-TPA** and at $\lambda = 331$ nm for ***S*-TPyA**, is formed at higher temperature from the molecularly dissolved solution. A second state begins to take part in the self-assembly process upon gradually lowering the temperature. Below a certain threshold, it dominates leading to a second state (state B), which shows a negative CD extremum, indicative of an inverted handedness.

For both systems the melting curves were measured at different concentrations up to 250 K to investigate how the temperature at which the inversion takes place (T_i) depends on the concentration. Whereas T_e is highly concentration-dependent, we observe that T_i is roughly invariant with the concentration (Figure 8). This result indicates that the conversion from state A to state B is a concentration-independent process. Typically such concentration-independent processes are related to intrahelical conformational changes or a transition between two types of assembled states,[38,39,52,53,54,55] making a bundling of supramolecular assemblies a less likely explanation for rationalizing the changes in the CD spectra.[56]

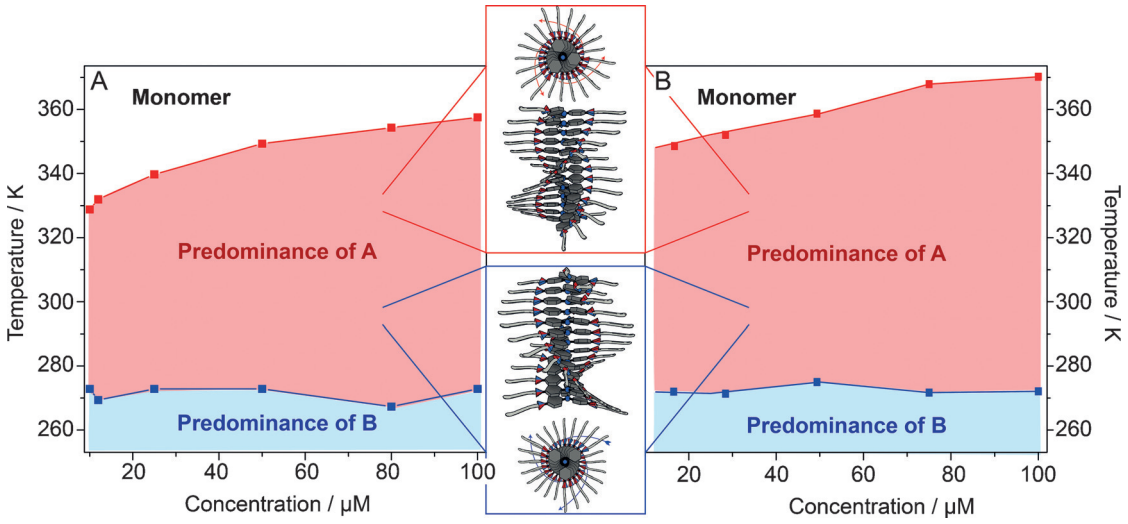

Figure 8. Diagram of states as a function of temperature and concentration. Elongation temperature (T_e, red squares) and inversion temperature (T_i, blue squares) of ***S*-TPA** in MCH (A) and ***S*-TPyA** in decalin (mixture of isomers) (B) recorded at different concentrations. Depending on temperature, both systems self-assemble in distinctly different aggregate states which show opposite handedness.

Discussion

The presence of two states, A and B, in both TPAs and TPyAs is supported by the computational analysis, which shows the possibility of two different self-assembled conformers with comparable energy. We propose that the pathway complexity observed experimentally is a delicate equilibrium between these two conformations. At high temperature, the free monomers can easily rotate around the single bonds (central nitrogen–aromatic ring and aromatic ring–amide) and no conformation is defined. However, as an effect of the decrease in thermal energy, the first small oligomers formed can have two conformations. Since the state A is formed through a cooperative process, the formation of nuclei with a defined conformation is crucial to achieve state A. We hypothesize that the formation of a 3:0 conformation is faster, and more 3:0 nuclei are formed, and hence the 3:0 conformation prevails over the 2:1 conformation at high temperature. Further lowering of the temperature and the concomitant increase in the length of the supramolecular aggregate lead to the 2:1 conformation becoming more stable. This leads to a sharp transition into thermodynamically stable state B.

The hypothesis that the molecules assume the 2:1 conformation in the B state explains the CD spectra of the two states: ***S*-TPA** shows almost mirror-image-related curves between state A and B, whereas ***S*-TPyA** does not (Figure 3A, 3C, 4C). We speculate that the origin of this difference lies in the higher molecular symmetry of TPA compared to that of TPyA. Indeed, the triphenylamine core maintains the C_3 symmetry in both 2:1 and 3:0 conformation, whereas the tripyridylamine core loses the C_3 axes in the 2:1 conformation (Figure 6). This effect is emphasized in decalin probably because of the higher conformational freedom of the side chains due to the presence of decalin isomers.

Our proposal is that the sharp transition from state A to state B is due to a conformational change within the monomer itself that leads to a transition within the supramolecular aggregate. This could explain both the transition from 3:0 to 2:1 and the resulting inversion of helicity, similarly to what has been reported by Bejagam et al.[57] Moreover, the internal conformational change justifies the invariance of T_i as a function of concentration (Figure 8). Nevertheless, based on the thermodynamic parameter determined here it is not possible to discriminate between direct or indirect conversion of the two states. Kinetic experiments are a prerequisite to identify the mechanism involved, being either an intra-stack conformational transition or a depolymerization–polymerization phenomenon.[58] Since hysteresis is a kinetic phenomenon we speculate that further studies, including simulations on the hysteresis will allow us to distinguish between the two possible scenarios.[59]

Conclusion

In conclusion, we showed that triarylamines bearing threefold hydrogen-bond units self-assemble in a strongly cooperative manner due to hydrogen-bonding interactions. In spite of the core differences, both molecules follow a general path affording helical supramolecular polymers, state A, at high temperature. Interestingly, the peculiar assembly of these triarylamines cannot be explained with a classical nucleation–elongation model down to the lower temperature, evidencing the presence of a second process that becomes more and more accessible at low temperatures, and results in a state B which shows an opposite handedness. The variable temperature CD analysis in a broader temperature window shows that small deviations observed at high temperature can be better studied by lowering the temperature; this opens the possibility to access states that otherwise would not be stable at higher temperatures. The hysteresis behavior that occurs upon thermal treatment allows one to synthesize and isolate different coexisting structures at the same temperature that can be used to modulate a supramolecular living polymerization.[31,32]

In addition, the CD inversion suggests that the two states have opposite helicity and, supported by computational calculation, we speculate that the reason for that is a molecular conformational inversion coupled to a helical inversion. This hypothesis indeed can explain the difference observed between the more symmetric ***S*-TPA** and the ***S*-TPyA**. In addition to that, another question still needs to be solved. All the recently proposed models[31,30,60] for assembled-state transitions propose a depolymerization–polymerization model. In our examined case, the inversion is drastic and sharp, which also suggests an internal polymer inversion, further supporting the hypothesis of an internal conformational change. Future experiments will focus on obtaining a better understanding of the origin of the observed hysteresis to obtain a deeper insight in the equilibria between the two states.

Acknowledgements

We like to thank Daan van der Zwaag at the Eindhoven University of Technology for fruitful discussions about pathway complexity. This project has received funding from the European Union's Horizon 2020 research and innovation program under the Marie Sklodowska-Curie grant agreement No 642083.

Keywords: CD inversion · handeness inversion · pathway complexity · supramolecular polymerization · triphenylamine

[1] C. K. Song, K. A. Luck, N. Zhou, L. Zeng, H. M. Heitzer, E. F. Manley, S. Goldman, L. X. Chen, M. A. Ratner, M. J. Bedzyk, R. P. H. Chang, M. C. Hersam, T. J. Marks, *J. Am. Chem. Soc.* **2014**, *136*, 17762 – 17773.
[2] M. Chen, H. Nie, B. Song, L. Li, J. Z. Sun, A. Qin, B. Z. Tang, *J. Mater. Chem. C* **2016**, *4*, 2901 – 2908.
[3] T. Yamada, H. Kaji, *J. Mol. Struct.* **2009**, *927*, 82 – 87.
[4] Y. T. Tsai, C. T. Lai, R. H. Chien, J. L. Hong, A. C. Yeh, *J. Polym. Sci. Part A Polym. Chem.* **2012**, *50*, 237 – 249.
[5] E. Bacher, M. Bayerl, P. Rudati, N. Reckefuss, C. D. Müller, K. Meerholz, O. Nuyken, *Macromolecules* **2005**, *38*, 1640 – 1647.
[6] H.-J. Yen, G.-S. Liou, *Polym. J.* **2016**, *48*, 117 – 138.
[7] Q. Liu, K. Jiang, L. Wang, Y. Wen, J. Wang, Y. Ma, Y. Song, *Appl. Phys. Lett.* **2010**, *96*, 213305.
[8] X. Jiang, K. M. Karlsson, E. Gabrielsson, E. M. J. Johansson, M. Quintana, M. Karlsson, L. Sun, G. Boschloo, A. Hagfeldt, *Adv. Funct. Mater.* **2011**, *21*, 2944 – 2952.

[9] N. Nath Ghosh, A. Chakraborty, S. Pal, A. Pramanik, P. Sarkar, *Phys. Chem. Chem. Phys.* **2014**, *16*, 25280 – 25287.
[10] A. Mahmood, *Sol. Energy* **2016**, *123*, 127 – 144.
[11] S. Paek, N. Cho, S. Cho, J. K. Lee, J. Ko, *Org. Lett.* **2012**, *14*, 6326 – 6329.
[12] M. Sonntag, K. Kreger, D. Hanft, P. Strohriegl, S. Setayesh, D. de Leeuw, *Chem. Mater.* **2005**, *17*, 3031 – 3039.
[13] S. T. Hoffmann, F. Jaiser, A. Hayer, H. Bässler, T. Unger, S. Athanasopoulos, D. Neher, A. Köhler, *J. Am. Chem. Soc.* **2013**, *135*, 1772 – 1782.
[14] A. B. Kaiser, *Adv. Mater.* **2001**, *13*, 927 – 941.
[15] A. C. Arias, J. D. MacKenzie, I. McCulloch, J. Rivnay, A. Salleo, *Chem. Rev.* **2010**, *110*, 3 – 24.
[16] A. P. H. J. Schenning, E. W. Meijer, *Chem. Commun.* **2005**, 3245 – 3258.
[17] A. Jain, S. J. George, *Mater. Today* **2015**, *18*, 206 – 214.
[18] A. P. H. J. Schenning, P. Jonkheijm, F. J. M. Hoeben, J. van Herrikhuyzen, S. C. J. Meskers, E. W. Meijer, L. M. Herz, C. Daniel, C. Silva, R. T. Phillips, *Synth. Met.* **2004**, *147*, 43 – 48.
[19] E. W. Meijer, A. P. H. J. Schenning, *Nature* **2002**, *419*, 353 – 354.
[20] T. Aida, E. W. Meijer, S. I. Stupp, *Science* **2012**, *335*, 813 – 817.
[21] M. Sofos, J. Goldberger, D. Stone, J. E. Allen, Q. Ma, D. J. Herman, W.-W. Tsai, L. J. Lauhon, S. I. Stupp, *Nat. Mater.* **2009**, *8*, 68 – 75.
[22] J. J. Armao, M. Maaloum, T. Ellis, G. Fuks, M. Rawiso, E. Moulin, N. Giuseppone, *J. Am. Chem. Soc.* **2014**, *136*, 11382 – 11388.
[23] Y. Domoto, E. Busseron, M. Maaloum, E. Moulin, N. Giuseppone, *Chem. Eur. J.* **2015**, *21*, 1938 – 1948.
[24] V. Faramarzi, F. Niess, E. Moulin, M. Maaloum, J.-F. Dayen, J.-B. Beaufrand, S. Zanettini, B. Doudin, N. Giuseppone, *Nat. Chem.* **2012**, *4*, 485 – 490.
[25] I. Nyrkova, E. Moulin, J. J. Armao, M. Maaloum, B. Heinrich, M. Rawiso, F. Niess, J.-J. Cid, N. Jouault, E. Buhler, *ACS Nano* **2014**, *8*, 10111 – 10124.
[26] J. Kim, J. Lee, W. Y. Kim, H. Kim, S. Lee, H. C. Lee, Y. S. Lee, M. Seo, S. Y. Kim, *Nat. Commun.* **2015**, *6*, 6959.
[27] P. Jonkheijm, P. van der Schoot, A. P. H. J. Schenning, E. W. Meijer, *Science* **2006**, *313*, 80 – 83.
[28] I. V. Baskakov, G. Legname, M. A. Baldwin, S. B. Prusiner, F. E. Cohen, *J. Biol. Chem.* **2002**, *277*, 21140 – 21148.
[29] P. A. Korevaar, T. F. A. de Greef, E. W. Meijer, *Chem. Mater.* **2014**, *26*, 576 – 586.
[30] P. A. Korevaar, S. J. George, A. J. Markvoort, M. M. J. Smulders, P. A. J. Hilbers, A. P. H. J. Schenning, T. F. A. De Greef, E. W. Meijer, *Nature* **2012**, *481*, 492 – 496.
[31] S. Ogi, K. Sugiyasu, S. Manna, S. Samitsu, M. Takeuchi, *Nat. Chem.* **2014**, *6*, 188 – 195.
[32] S. Ogi, V. Stepanenko, K. Sugiyasu, M. Takeuchi, F. Würthner, *J. Am. Chem. Soc.* **2015**, *137*, 3300 – 3307.
[33] R. Rai, A. Saxena, A. Ohira, M. Fujiki, *Langmuir* **2005**, *21*, 3957 – 3962.
[34] D. van der Zwaag, T. F. A. de Greef, E. W. Meijer, *Angew. Chem. Int. Ed.* **2015**, *54*, 8334 – 8336; *Angew. Chem.* **2015**, *127*, 8452 – 8454.
[35] A. Aliprandi, M. Mauro, L. De Cola, *Nat. Chem.* **2015**, *8*, 10 – 15.
[36] J. Kang, D. Miyajima, T. Mori, Y. Inoue, Y. Itoh, T. Aida, *Science* **2015**, *347*, 646 – 651.
[37] S. Ogi, V. Stepanenko, J. Thein, F. Würthner, *J. Am. Chem. Soc.* **2016**, *138*, 670 – 678.
[38] Y. Nakano, A. J. Markvoort, S. Cantekin, I. A. W. Filot, H. M. M. ten Eikelder, E. W. Meijer, A. R. A. Palmans, *J. Am. Chem. Soc.* **2013**, *135*, 16497 – 16506.
[39] S. Cantekin, Y. Nakano, J. C. Everts, P. van der Schoot, E. W. Meijer, A. R. A. Palmans, *Chem. Commun.* **2012**, *48*, 3803 – 3805.
[40] R. D. Mukhopadhyay, A. Ajayaghosh, *Science* **2015**, *349*, 241 – 242.
[41] P. J. M. Stals, J. C. Everts, R. de Bruijn, I. A. W. Filot, M. M. J. Smulders, R. Martín-Rapún, E. A. Pidko, T. F. A. de Greef, A. R. A. Palmans, E. W. Meijer, *Chem. Eur. J.* **2010**, *16*, 810 – 821.
[42] P. J. M. Stals, M. M. J. Smulders, R. Martín-Rapún, A. R. A. Palmans, E. W. Meijer, *Chem. Eur. J.* **2009**, *15*, 2071 – 2080.
[43] M. M. J. Smulders, A. P. H. J. Schenning, E. W. Meijer, *J. Am. Chem. Soc.* **2008**, *130*, 606 – 611.
[44] K. Wei, J. Ni, Y. Min, S. Chen, Y. Liu, *Chem. Commun.* **2013**, *49*, 8220 – 8222.
[45] H. Szelke, H. Wadepohl, M. Abu-youssef, R. Krämer, *Eur. J. Inorg. Chem.* **2009**, 251 – 260.
[46] W. Yao, K. Kavallieratos, S. de Gala, R. H. Crabtree, *Inorg. Chim. Acta* **2000**, *311*, 45 – 49.
[47] J. Wang, C. He, P. Wu, J. Wang, C. Duan, *J. Am. Chem. Soc.* **2011**, *133*, 12402 – 12405.
[48] G. Koeckelberghs, L. De Cremer, W. Vanormelingen, W. Dehaen, T. Verbiest, A. Persoons, C. Samyn, *Tetrahedron* **2005**, *61*, 687 – 691.
[49] A. J. Markvoort, H. M. M. ten Eikelder, P. A. J. Hilbers, T. F. A. de Greef, E. W. Meijer, *Nat. Commun.* **2011**, *2*, 509.
[50] K. K. Bejagam, G. Fiorin, M. L. Klein, S. Balasubramanian, *J. Phys. Chem. B* **2014**, *118*, 5218 – 5228.
[51] I. A. W. Filot, A. R. A. Palmans, P. A. J. Hilbers, R. A. van Santen, E. A. Pidko, T. F. A. de Greef, *J. Phys. Chem. B* **2010**, *114*, 13667 – 13674.
[52] J. van Gestel, P. van der Schoot, M. A. J. Michels, *J. Phys. Chem. B* **2001**, *105*, 10691 – 10699.
[53] M. Roman, C. Cannizzo, T. Pinault, B. Isare, B. Andrioletti, P. van der Schoot, L. Bouteiller, *J. Am. Chem. Soc.* **2010**, *132*, 16818 – 16824.
[54] M. Bellot, L. Bouteiller, *Langmuir* **2008**, *24*, 14176 – 14182.
[55] P. van der Schoot, M. A. J. Michels, L. Brunsveld, R. P. Sijbesma, A. Ramzi, *Langmuir* **2000**, *16*, 10076 – 10083.
[56] P. J. M. Stals, P. A. Korevaar, M. A. J. Gillissen, T. F. A. de Greef, C. F. C. Fitié, R. P. Sijbesma, A. R. A. Palmans, E. W. Meijer, *Angew. Chem. Int. Ed.* **2012**, *51*, 11297 – 11301; *Angew. Chem.* **2012**, *124*, 11459 – 11463.
[57] K. K. Bejagam, C. Kulkarni, S. J. George, S. Balasubramanian, *Chem. Commun.* **2015**, *51*, 16049 – 16052.
[58] D. van der Zwaag, P. A. Pieters, P. A. Korevaar, A. J. Markvoort, A. J. H. Spiering, T. F. A. de Greef, E. W. Meijer, *J. Am. Chem. Soc.* **2015**, *137*, 12677 – 12688.
[59] R. Schulman, E. Winfree, *Proc. Natl. Acad. Sci. USA* **2007**, *104*, 15236 – 15241.
[60] S. Ogi, T. Fukui, M. L. Jue, M. Takeuchi, K. Sugiyasu, *Angew. Chem. Int. Ed.* **2014**, *53*, 14363 – 14367; *Angew. Chem.* **2014**, *126*, 14591 – 14595.

Manuscript received: August 18, 2016
Final Article published: December 16, 2016

